

## Interaction of Benzene with Transition Metal Cations: Theoretical Study of Structures, Energies, and IR Spectra

Hai-Bo Yi,<sup>\*,†</sup> Han Myoung Lee,<sup>\*,‡</sup> and Kwang S. Kim<sup>\*,§</sup>

*College of Chemistry and Chemical Engineering, Hunan University, Changsha, Hunan 410082, China, Department of Chemistry and Center for Basic Sciences, Pohang University of Science and Technology, Pohang 790-784, Korea, and Center for Superfunctional Materials, Department of Chemistry, Pohang University of Science and Technology, San 31, Hyojadong, Namgu, Pohang 790-784, Korea*

Received March 31, 2009

**Abstract:** The cation– $\pi$  interactions have been intensively studied. Nevertheless, the interactions of  $\pi$  systems with heavy transition metals and their accurate conformations are not well understood. Here, we theoretically investigate the structures and binding characteristics of transition metal (TM) cations including novel metal cations ( $\text{TM}^{n+} = \text{Cu}^+, \text{Ag}^+, \text{Au}^+, \text{Pd}^{2+}, \text{Pt}^{2+}$ , and  $\text{Hg}^{2+}$ ) interacting with benzene (Bz). For comparison, the alkali metal complex of  $\text{Na}^+$ –Bz is also included. We employ density functional theory (DFT) and high levels of ab initio theory including Møller–Plesset second-order perturbation (MP2) theory, quadratic CI method with single and double substitutions (QCISD), and the coupled cluster theory with single, double, and perturbative triple excitations (CCSD(T)). Each of the transition metal complexes of benzene exhibits intriguing binding characteristics, different from the typical cation– $\pi$  interactions between alkali metal cations and aromatic rings. The complexes of  $\text{Na}^+$ ,  $\text{Cu}^+$ , and  $\text{Ag}^+$  favor the conformation of  $C_{6v}$  symmetry with the cation above the benzene centroid ( $\pi_{\text{cen}}$ ). The formation of these complexes is attributed to the electrostatic interaction, while the magnitude of charge transfer has little correlation with the total interaction energy. Because of the  $\text{TM}^{n+} \leftarrow \pi$  donation, cations  $\text{Au}^+$ ,  $\text{Pd}^{2+}$ ,  $\text{Pt}^{2+}$ , and  $\text{Hg}^{2+}$  prefer the off-center  $\pi$  conformation ( $\pi_{\text{off}}$ ) or the  $\pi$  coordination to a C atom of the benzene. Although the electrostatic interaction is still important, the  $\text{TM} \leftarrow \pi$  donation effect is responsible for the binding site. The  $\text{TM}^{n+}$ –Bz complexes give some characteristic IR peaks. The complexes of  $\text{Na}^+$ ,  $\text{Cu}^+$ , and  $\text{Ag}^+$  give two IR active modes between 800 and 1000  $\text{cm}^{-1}$ , which are inactive in the pure benzene. The complexes of  $\text{Au}^+$ ,  $\text{Pd}^{2+}$ ,  $\text{Pt}^{2+}$ , and  $\text{Hg}^{2+}$  give characteristic peaks for the ring distortion, C–C stretching, and C–H stretching modes as well as significant red-shifts in the CH out-of-plane bending.

### 1. Introduction

Cation– $\pi$  interactions have been characterized in a wide range of contexts,<sup>1–4</sup> due to the importance in diverse fields of

chemistry,<sup>5</sup> biology,<sup>6</sup> and nanotechnology.<sup>7</sup> A number of studies have been reported on the binding of alkali metal cations or organic cations with ethylene, acetylene, benzene, or other  $\pi$  systems. These interaction forces have been utilized to design ionophores and receptors.<sup>8</sup> Benzene (Bz) is a good prototype aromatic compound and serves as a model for the  $\pi$  systems. Alkali metal cations prefer the formation of  $\pi$  complexes of  $C_{6v}$  symmetry.<sup>9</sup> As transition metal arene complexes that are key intermediates in aromatic C–H bond activation display multifaceted coordination chemistry,<sup>11</sup> transition metal complexes with aromatic compounds have been widely investi-

\* Corresponding author e-mail: hby1@hnu.cn (H.-B.Y.); abcd01hm@postech.ac.kr (H.M.L.); kim@postech.ac.kr (K.S.K.).

<sup>†</sup> Hunan University.

<sup>‡</sup> Department of Chemistry and Center for Basic Sciences, Pohang University of Science and Technology.

<sup>§</sup> Department of Chemistry, Pohang University of Science and Technology.

gated,<sup>10</sup> and the interactions of novel metals ( $\text{Cu}^+$ ,  $\text{Ag}^+$ , and  $\text{Au}^+$ ) with Bz have been reported.<sup>12</sup>

Recently, the interest in gas-phase reactions for metal dications has grown<sup>13–15</sup> due to advances in experimental techniques such as electrospray ionization and electron impact double ionization, which permit the generation of dication in the gas phase. Using NMR spectroscopy, Johansson et al. detected a  $\text{Pt}^{2+}$ –benzene complex,  $[(\text{dimine})\text{Pt}(\eta^2\text{-C}_6\text{H}_6)\text{CH}_3]^+$ , a precursor to arene C–H oxidative addition.<sup>15</sup> Templeton and co-workers gave further structural characterization for the  $\text{Pt}^{2+}$   $\eta^2$ -benzene adduct.<sup>16</sup> In this regard, a further detailed investigation of binding features of the  $\text{TM}^{n+}$ –Bz complexes would be of importance.

It is known that the interaction of alkali–metal cations with Bz is mainly governed by the electrostatic and induction interactions.<sup>1,5,17</sup> In the interactions of olefinic, aromatic, and heteroaromatic  $\pi$  systems with alkali metal ions<sup>5</sup> and also in the  $(\text{C}_2\text{H}_4\text{--TM})^+$  complexes,<sup>18,19</sup> the electrostatic interaction also plays an important role. However, molecular dications formed by attachment of a  $\text{TM}^{2+}$  dication to a neutral base often show significant bonding features. Thus, it is important to understand the role of ionic/covalent bonding in the formation of a  $\text{TM}^{2+}$ – $\pi$  cluster.

In this study, we investigate the bindings of  $\text{Pd}^{2+}$ ,  $\text{Pt}^{2+}$ , and  $\text{Hg}^{2+}$  with Bz using ab initio theory and density functional theory, and we also report the bindings of  $\text{Na}^+$ ,  $\text{Cu}^+$ ,  $\text{Ag}^+$ , and  $\text{Au}^+$  with Bz for comparison. It is vital to understand these interactions for the design and development of the receptors and sensors for the heavy transition metal recognition as well as the hazardous biological problems of the heavy transition metal intercalation between DNA stacks, which have been hot topics in molecular/biomolecular recognition study of heavy metals.

The formation of  $\text{TM}^{n+}$ –Bz complexes is often associated with charge transfer from  $\text{TM}^{n+}$  to Bz. The charge transfer affects the binding feature and structural distortion of  $\pi$  moieties. Both geometrical and electronical (i.e., charge-transfer/polarization) changes due to the complexation of  $\text{TM}^{n+}$  with Bz result in significant changes in IR spectra. Thus, to facilitate the experiments for the structural information of  $\text{TM}^{n+}$ – $\pi$  complexes, we also compare the differences in IR spectra between different transition metal complexes.

## II. Methods

Many possible structures of  $\text{TM}^{n+}$ –Bz complexes were optimized using DFT calculations [Becke three parameters with the Lee–Yang–Parr functional (B3LYP) and the Perdew, Burke, and Ernzerhof functional (PBE)] and ab initio calculations [Möller Plesset second-order perturbation theory (MP2), and quadratic CI method including single and double substitutions (QCISD)].<sup>20</sup> The basis set for benzene was used with the aug-cc-pVDZ (aVDZ) basis set. The pseudopotentials of transition metals (Cu, Ag, Au, Pd, Pt, and Hg) were used with the Stuttgart RSC 1997 effective core potential (ECP).<sup>21</sup> For Au, Pd, Pt, and Hg, the relativistic effective core potentials (RECP) developed by the Stuttgart group were used in conjunction with the basis set to describe the metal valence electrons. For Na, the cc-pCVDZ basis set was used, and a single f function was added for Cu, Ag,

and Au.<sup>22</sup> The binding energies were further calculated using the coupled cluster theory with single, double, and perturbative triple excitations (CCSD(T)) employing the aVDZ basis set and the MP2 theory using the aug-cc-pVTZ (aVTZ) basis set (for benzene) on the MP2/aVDZ optimized geometries. In this aVTZ case, the cc-pCVTZ basis set was used for Na, and a set of two f and one g polarization functions were added for transition metals (Cu, Ag, Au, Pd, Pt, and Hg), as suggested by Martin and Sundermann.<sup>23</sup> The basis set superposition error (BSSE) correction was taken into account. The complete basis set (CBS) limit values for the MP2 binding energies were evaluated on the basis of the extrapolation method to exploit that the electron correlation error is proportional to  $N^{-3}$  for the aug-cc-pVNZ basis set.<sup>24</sup> Given that the difference in binding energy between MP2 and CCSD(T) for the same basis set does not change significantly with increasing basis set size, the CCSD(T)/CBS binding energies were evaluated from the MP2/CBS ones by applying the difference between CCSD(T) and MP2 binding energies for the aug-cc-pVDZ basis set.<sup>24b</sup> QCISD calculations were carried out using the 6-31G\*\* basis set, with the relativistic effective core potentials (RECP) and the corresponding basis set for transition metals. All calculations in this work were carried out using a suite of Gaussian 03 programs.<sup>25</sup> Molecular orbital analysis was done on the basis of the MP2 calculations by using the POSMOL package.<sup>26</sup>

## III. Results

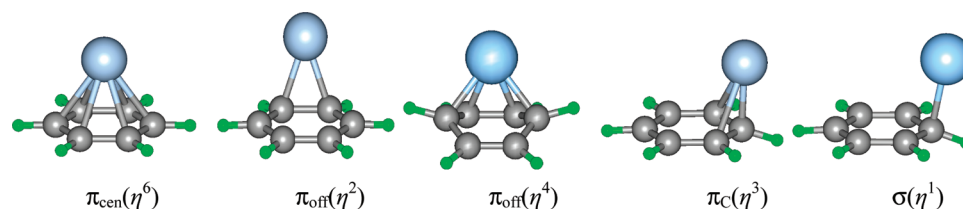
**A. TM Cations and Benzene.** Novel metals ( $\text{Cu}^+$ ,  $\text{Ag}^+$ , and  $\text{Au}^+$ ) as well as alkali metal  $\text{Na}^+$  have singlet ground states, and their complexes also have singlet ground states.  $\text{Pd}^{2+}$  and  $\text{Pt}^{2+}$  have triplet ground states of the  $d^8$  type with electronic configurations of  $4d^8$  and  $4f^{14}5d^8$ , respectively. The  $\text{Pd}^{2+}$ –Bz and  $\text{Pt}^{2+}$ –Bz complexes may exist in either the triplet or singlet state.  $\text{Hg}^{2+}$  is of the  $d^{10}$  type with an electronic configuration of  $4f^{14}5d^{10}$ ; thus, the  $\text{Hg}^{2+}$  complexes are mainly closed shell systems with the singlet ground state. The “5d” atomic orbitals (AOs) of  $\text{Hg}^{2+}$  are fully occupied, so that the interactions of  $\text{Hg}^{2+}$  with  $\pi$  ligands would be quite different from those of  $\text{Pd}^{2+}$  and  $\text{Pt}^{2+}$ .

For the ionization potentials (IP) of neutral metals, the B3LYP/aVDZ and PBE/aVDZ values are slightly overestimated, while QCISD/aVTZ values are slightly underestimated. The MP2/aVTZ and CCSD(T)/aVTZ values are in good agreement with the experimental values (except for the case of Hg),<sup>27</sup> as listed in Table 1. However, as for the electron affinity (EA), the B3LYP/aVDZ and PBE/aVDZ values are in reasonable agreement with the experimental values,<sup>27</sup> the MP2/aVTZ values are slightly underestimated, and the CCSD(T)/aVTZ values are very close to the experimental values except for the case of Hg. Because of the relativistic effects, the energy of 6s is lowered, and the energy splitting between “5d” and “6s” AOs of Au is much smaller than that between “4d” and “5s” AOs of Ag. As a result, the IP value of Au is much larger than those of Cu and Ag. Similarly, the large IP of Pt or Hg is also attributed to the relativistic effect. Despite that the CCSD(T)/aVTZ well reproduces the experimental

**Table 1.** Ionization Potential (IP) and Electron Affinities (EA) for TM = Na, Cu, Ag, Au, Pd, Pt, and Hg (in eV at the B3LYP/aVDZ, MP2/aVTZ, and CCSD(T)/aVTZ Levels)<sup>a</sup>

	conf.	IP						EA						d-s gap <sup>b</sup>
		B3LYP	PBE	MP2	CCSD(T)	QCISD	expt.	B3LYP	PBE	MP2	CCSD(T)	QCISD	expt.	
Na	2p <sup>10</sup> 3s <sup>1</sup>	5.40	5.33	5.07	5.08	4.95	5.14	0.59	0.56	0.21	0.44	0.53	0.55	
Cu	3d <sup>10</sup> 4s <sup>1</sup>	8.03	8.15	7.59	7.38	7.49	7.73	1.00	1.02	0.81	0.86	1.05	1.24	1.56
Ag	4d <sup>10</sup> 5s <sup>1</sup>	7.97	8.05	7.47	7.41	7.33	7.57	1.38	1.39	1.00	1.18	1.09	1.30	3.55
Au	5d <sup>10</sup> 6s <sup>1</sup>	9.33	9.42	9.13	8.93	8.83	9.23	2.21	2.28	2.18	2.07	1.93	2.31	1.89
Pd	4d <sup>10</sup>	8.70	8.80	8.62	8.14	8.03	8.34	0.77	0.92	0.24	0.39	0.32	0.56	2.51
Pt	5d <sup>9</sup> 6s <sup>1</sup>	9.25	9.36	9.08	8.80	8.74	9.00	1.39	1.98	1.25	1.91	0.89	2.13	1.01
Hg <sup>c</sup>	5d <sup>10</sup> 6s <sup>2</sup>	9.70	9.23	9.63	9.49	9.37	10.44	-0.22	-0.20	-0.46	-0.84	-0.45	0	5.17 <sup>c</sup>

<sup>a</sup> The experimental IP and EA values are from ref 27. <sup>b</sup> Energy gap between  $(n-1)d$  and  $ns$  orbitals. <sup>c</sup> Inert-pair effect of 6s<sup>2</sup>.

**Figure 1.** Binding sites of TM<sup>n+</sup> for Bz.

IP and EA of various metals in a very consistent manner, it gives significant deviation in the IP and EA only for Hg possibly due to the basis set insufficiency. Nevertheless, the structure and binding energy for the Hg<sup>2+</sup>-benzene complex would still be reliable because the binding energy reflects the cancellation effect of errors and the basis set would not be insufficient for Hg<sup>2+</sup>, which has two electrons less than Hg (even though it is insufficient for Hg). The s-d energy splitting of Hg is particularly large due to the insignificant spin-orbital coupling because Hg has full 5d and 6s valence shells. In the case of Pd<sup>2+</sup>/Pt<sup>2+</sup>, an electron from a singly occupied “d” AO can be promoted to an unoccupied “s” AO, which makes it possible a  $\pi \leftarrow d$  donation for Pd<sup>2+</sup>/Pt<sup>2+</sup>- $\pi$  complexes.

**B. TM<sup>n+</sup>-Benzene Complexes: Conformation.** We have investigated several different conformations for the binding of TM<sup>n+</sup> with Bz using B3LYP/aVDZ and MP2/aVDZ calculations. The conformations for these complexes can be classified into five different binding types [ $\pi_{\text{cen}}(\eta^6)$ ,  $\pi_{\text{off}}(\eta^4)$ ,  $\pi_{\text{off}}(\eta^2)$ ,  $\pi_{\text{C}}(\eta^3)$ , and  $\sigma_{\text{C}}(\eta^1)$ ], as shown in Figure 1. In the case of  $\pi_{\text{cen}}$ , the TM is above the ring centroid, interacting with six carbon atoms,  $\eta^6$ . For  $\pi_{\text{off}}$ , the TM is above the center of a carbon bond ( $\eta^2$ ) or above two carbon bonds ( $\eta^4$ ). In the case of  $\pi_{\text{C}}$ , the TM is above three carbon atoms of Bz ( $\eta^3$ ). For  $\sigma$ , the TM is above one carbon atom of Bz ( $\eta^1$ ). The binding of Na<sup>+</sup> with Bz is also reported for comparison. For convenience's sake, we put Na in TM in terms of notation. For the binding of TM<sup>n+</sup> to Bz, the Na<sup>+</sup> cation favors the  $\pi_{\text{cen}}$  conformation. The Cu<sup>+</sup> cation can change the position above the whole Bz plane, as can be noted from very small differences between different conformations, and, accordingly, the lowest energy conformation depends on the calculation level of theory. At the MP2/aVDZ level, the  $\pi_{\text{cen}}$  structure is slightly more favored. For the Ag<sup>+</sup> cation, B3LYP/aVDZ, PBE/aVDZ, and QCISD/6-31G\*\* favor the  $\pi_{\text{off}}$  and  $\pi_{\text{C}}$  structures, but MP2/aVDZ favors the  $\pi_{\text{cen}}$  structure. The Au<sup>+</sup> cation favors the  $\pi_{\text{off}}$  structure. The Pd<sup>2+</sup>

and Pt<sup>2+</sup> cations favor the  $\pi_{\text{off}}$  conformation for the singlet state and the  $\pi_{\text{cen}}$  conformation for the triplet state.

The structures of the TM<sup>n+</sup>-Bz complexes at the MP2/aVDZ level are given in Figure 2. Upon the complexation ( $\pi_{\text{cen}}$ ) of the benzene with Na<sup>+</sup>, Cu<sup>+</sup>, and Ag<sup>+</sup>, the C-C bond lengths are slightly increased (by 0.005, 0.017, and 0.012 Å, respectively). In the  $\pi_{\text{off}}(\eta^2)$  complexes of Au<sup>+</sup>, one C-C bond length increases up to 1.461 Å, while in the  $\pi_{\text{off}}(\eta^4)$  complexes of Pd<sup>2+</sup> and Pt<sup>2+</sup>, four C-C bond lengths increase up to 1.466–1.467 and 1.473–1.480 Å, respectively. For the Hg<sup>2+</sup> complex, the  $\pi_{\text{C}}(\eta^3)$  is slightly more favored than  $\pi_{\text{off}}(\eta^4)$ . The  $\pi_{\text{off}}$  and  $\pi_{\text{C}}$  conformers have some of the covalent characters (i.e.,  $\sigma$  conformers), which are similar to the protonated Bz complex.<sup>28</sup>

The binding energies of TM<sup>n+</sup>-Bz complexes are in Table 2. The Na<sup>+</sup>-Bz system has been investigated intensively at various theoretical levels.<sup>29</sup> The most stable structure of Na<sup>+</sup>-Bz is of  $C_{6v}$  symmetry, the B3LYP/aVDZ binding energy is 20.4 kcal/mol, and the MP2/CBS value is 21.7 kcal/mol. The CCSD(T)/CBS value (22.1 kcal/mol) is in excellent agreement with the experimental value (22.1 kcal/mol).<sup>30</sup> For the Cu<sup>+</sup>-Bz complex, the B3LYP/aVDZ and PBE/aVDZ binding energies of  $\pi_{\text{cen}}$ ,  $\pi_{\text{off}}$ , and  $\pi_{\text{C}}$  structures are nearly same, whereas at the MP2/aVDZ and QCISD/6-31G\* levels only the  $\pi_{\text{cen}}$  structure is stable. For the Ag<sup>+</sup>-Bz complex, the B3LYP/aVDZ, PBE/aVDZ, and QCISD(T)/6-31G\* binding energies of the  $\pi_{\text{off}}$  and  $\pi_{\text{C}}$  structures are greater than that of  $\pi_{\text{cen}}$  structure, whereas at the MP2/aVDZ, MP2/CBS, and CCSD(T)/CBS levels only the  $\pi_{\text{cen}}$  structure is stable. For the Au<sup>+</sup>-Bz complex, the  $\pi_{\text{C}}$  and  $\pi_{\text{off}}$  structures are similar in energy, which are much more stable than the  $\pi_{\text{cen}}$  structure. Although the B3LYP/aVDZ, MP2/aVDZ, and CCSD(T)/aVDZ binding energies are underestimated, the PBE/aVDZ and MP2/CBS binding energies are overestimated, and the MP2/aVTZ and CCSD(T)/CBS binding energies are in good agreement with the experimental values. The QCISD/6-31G\*\* binding energy of Na<sup>+</sup>-Bz agrees well with the experimental values, while the QCISD/6-31G\*\*

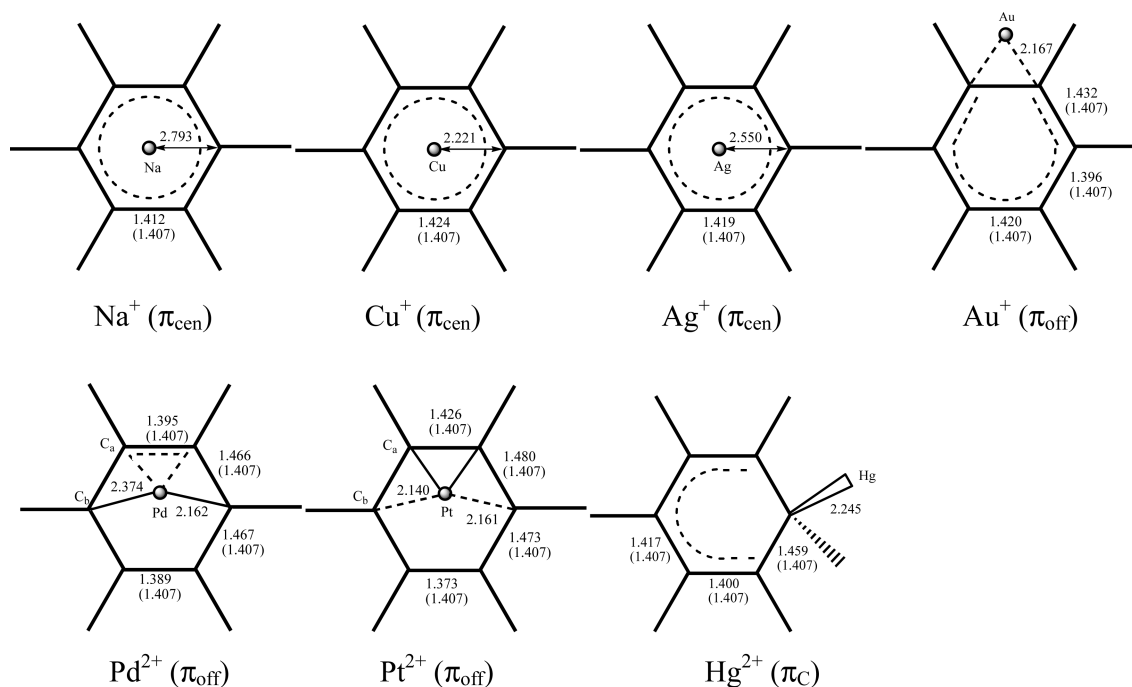


**Figure 2.** Most stable  $\text{TM}^{n+}$ -Bz complexes at the MP2/aVDZ level. Bond lengths are in angstroms. The C-C bond length of the uncomplexed Bz is 1.407 Å.

calculations apparently underestimate those of  $\text{Cu}^+$ -Bz and  $\text{Au}^+$ -Bz.  $\text{Pt}^{2+}$  has the singlet ground state due to its bonding feature. However, for  $\text{Pd}^{2+}$ -Bz, the triplet state of the  $\pi_{\text{cen}}$  structure is more stable at the B3LYP, PBE, and QCISD levels, while the singlet state of the  $\pi_{\text{off}}$  structure is more stable at the MP2/aVDZ, MP2/aVTZ, MP2/CBS, CCSD(T)/aVDZ, and CCSD(T)/CBS levels. Thus, at the present level of theory, the  $\pi_{\text{off}}$  structure is more likely, but for clear conclusion, this structure needs to be further investigated at much higher levels of theory in the future.

The vibrational frequencies of Bz were calculated using B3LYP/aVDZ, MP2/aVDZ, and QCISD/6-31G\*\* (Table 3 and Figure 3). At the MP2/aVDZ level, the strong peaks at 678, 1052, 1469, and 3229  $\text{cm}^{-1}$  are assigned as an out-of-plane H bending mode, an in-plane H bending mode, a ring distortion mode, and a CH stretching mode, respectively, which correspond to the strong experimental bands observed at 673, 1038, 1469, and 3210  $\text{cm}^{-1}$  by Jaeger et al.<sup>33</sup>

**C. Binding Characteristics of the  $\text{TM}^{n+}$  Cation with Benzene.** As compared to the nonpolarizable cation  $\text{Na}^+$ , the binding energy of  $\text{Cu}^+$ ,  $\text{Ag}^+$ , or  $\text{Au}^+$  with Bz is relatively large. However, the formation of  $\text{TM}^{n+}$ -Bz complexes often shows significant bonding characteristics associated with the charge transfer from  $\text{TM}^{n+}$  to Bz. The atomic charges were calculated using MP2/aVTZ calculations based on the natural bond orbital (NBO) population analysis (Table 4).

**C1. Binding of  $\text{Na}^+$ ,  $\text{Cu}^+$ , and  $\text{Ag}^+$  to Benzene.**  $\text{Cu}^+$  and  $\text{Ag}^+$  have the electron configuration of  $d^{10}$ , and so the  $\text{TM}-\pi$  donation in these complexes would not be significant. The experimental IP values of Cu and Ag are 7.73 and 7.57 eV,<sup>27</sup> respectively (7.59 and 7.47 eV at the MP2/aVTZ level, respectively). The experimental IP of Bz is 9.3 eV<sup>35</sup> (9.11 eV at the MP2/aVTZ level), and thus the donation from the  $\pi$  electrons of Bz to the unoccupied s orbital would not be favorable. Based on the NBO charge population, the charge

transfer from  $\text{Cu}^+$  or  $\text{Ag}^+$  to Bz is insignificant (Table 4). Thus, the binding between Bz and  $\text{Na}^+/\text{Cu}^+/\text{Ag}^+$  is attributed to the electrostatic and inductive energies, and this binding decreases with increasing distance between the metal cation and the Bz centroid.

The binding of  $\text{Na}^+$ ,  $\text{Cu}^+$ , or  $\text{Ag}^+$  with Bz brings about IR spectral changes of the Bz moiety. Figure 4 shows the MP2/aVDZ IR spectra of the  $\text{TM}^{n+}$ -Bz complexes as compared to the pure benzene. As we discussed earlier, for the pure Bz, a CH out-of-plane bending mode appears at 678  $\text{cm}^{-1}$ , a CH in-plane bending mode at 1052  $\text{cm}^{-1}$ , a ring distortion mode at 1469  $\text{cm}^{-1}$ , and a CH stretching mode at 3229  $\text{cm}^{-1}$ . For the  $\text{Na}^+$ -Bz complex, two low frequencies at 726 and 886  $\text{cm}^{-1}$  are out-of-plane bending modes, which are blue-shifted. The symmetric ring breathing mode appears at 996  $\text{cm}^{-1}$ , the in-plane H bending mode at 1046  $\text{cm}^{-1}$ , and the ring distorting mode at 1452  $\text{cm}^{-1}$ . The IR spectra of  $\text{Cu}^+$ -Bz and  $\text{Ag}^+$ -Bz complexes are similar to those of the  $\text{Na}^+$ -Bz complex, while the significant difference is that the C-H stretching mode is IR inactive for the  $\text{Na}^+$ -Bz complex, which is due partly to the polarization of C-H bond reduced by the interaction between  $\text{Na}^+$  and benzene.

**C2. Binding of  $\text{Au}^+$ ,  $\text{Pd}^{2+}$ ,  $\text{Pt}^{2+}$ , and  $\text{Hg}^{2+}$  to Benzene.** Because the effective ionic radii for octa-coordinated  $\text{Li}^+$ ,  $\text{Na}^+$ , and  $\text{K}^+$  are 0.92, 1.16, and 1.51 Å,<sup>36</sup> respectively, the electrostatic interaction contribution in the Bz complexes with an alkali metal cation decreases as the distance between the metal cation and the Bz centroid increases. However, such a trend is not observed for the Bz complexes with  $\text{Cu}^+$ ,  $\text{Ag}^+$ , and  $\text{Au}^+$ . The effective ionic radii for hexa-coordinated  $\text{Cu}^+$ ,  $\text{Ag}^+$ , and  $\text{Au}^+$  are 0.77, 1.15, and 1.37 Å. Because of the strong electron affinity of  $\text{Au}^+$ , the binding of  $\text{Au}^+$  with Bz is clearly stronger than those of  $\text{Cu}^+$  and  $\text{Ag}^+$ . Unlike those of  $\text{Na}^+$ ,  $\text{Cu}^+$ , and  $\text{Ag}^+$ , the charge transfer from  $\text{Au}^+$  to Bz is significant ( $q(\text{Bz}) = 0.21$ ). The NBO analysis shows that



**Table 2.** BSSE-Corrected B3LYP, PBE, MP2, QCISD, and CCSD(T) Binding Energies (kcal/mol) of the  $\text{TM}^{n+}$ -Bz Complexes<sup>a</sup>

	B3LYP/aVDZ			PBE/aVDZ			MP2/aVDZ			QCISD/6-31G**		
	$\pi_{\text{cent}}(\eta^6)$	$\pi_{\text{c}}(\eta^3)$	$\pi_{\text{off}}(\eta^4)$	$\pi_{\text{cent}}(\eta^6)$	$\pi_{\text{c}}(\eta^3)$	$\pi_{\text{off}}(\eta^4)$	$\pi_{\text{cent}}(\eta^6)$	$\pi_{\text{c}}(\eta^3)$	$\pi_{\text{off}}(\eta^4)$	$\pi_{\text{cent}}(\eta^6)$	$\pi_{\text{c}}(\eta^3)$	$\pi_{\text{off}}(\eta^4)$
$^1(\text{Na}-\text{Bz})^+$	20.4			24.3			21.7			23.8		
$^1(\text{Cu}-\text{Bz})^+$	50.9	50.4	50.7	63.6	63.6	63.6	52.2			44.1	44.1	44.1
$^1(\text{Ag}-\text{Bz})^+$	34.5	38.8	38.9	40.9	45.4	45.8	35.1			31.0	31.8	31.9
$^1(\text{Au}-\text{Bz})^+$	41.4	58.9	58.4	50.3	69.7	69.7	47.9			29.5	46.5	46.2
$^1(\text{Pd}-\text{Bz})^{2+}$		186.8	186.9		213.3	213.9					159.5	162.8
$^1(\text{Pt}-\text{Bz})^{2+}$		203.3	203.7		228.1	231.1					173.2	177.1
$^1(\text{Hg}-\text{Bz})^{2+}$	128.1	150.8	148.4	143.1	163.6	161.5	114.1			108.4	120.0	117.8
$^3(\text{Pd}-\text{Bz})^{2+}$	198.5			218.4			164.7			169.1		
$^3(\text{Pt}-\text{Bz})^{2+}$	200.0			224.9			177.9			172.2		
	MP2/aVTZ//MP2/aVDZ			MP2/CBS//MP2/aVDZ			CCSD(T)/aVDZ//MP2/aVDZ			CCSD(T)/CBS//MP2/aVDZ		
	$\pi_{\text{cent}}(\eta^6)$	$\pi_{\text{c}}(\eta^3)$	$\pi_{\text{off}}(\eta^4)$	$\pi_{\text{cent}}(\eta^6)$	$\pi_{\text{c}}(\eta^3)$	$\pi_{\text{off}}(\eta^4)$	$\pi_{\text{cent}}(\eta^6)$	$\pi_{\text{c}}(\eta^3)$	$\pi_{\text{off}}(\eta^4)$	$\pi_{\text{cent}}(\eta^6)$	$\pi_{\text{c}}(\eta^3)$	$\pi_{\text{off}}(\eta^4)$
$^1(\text{Na}-\text{Bz})^+$	21.7			21.7			22.1			22.1		
$^1(\text{Cu}-\text{Bz})^+$	59.7			62.9			44.1			56.0		
$^1(\text{Ag}-\text{Bz})^+$	40.9			43.5			31.4			40.1		
$^1(\text{Au}-\text{Bz})^+$	55.9	68.9	69.7	52.9	72.1	73.1	39.6			50.9	63.6	64.3
$^1(\text{Pd}-\text{Bz})^{2+}$		190.5	205.5		206.5	222.7					204.1	215.4
$^1(\text{Pt}-\text{Bz})^{2+}$		221.8	230.7		241.3	251.3					237.4	243.4
$^1(\text{Hg}-\text{Bz})^{2+}$	134.4	143.8	142.9	142.9	152.8	151.7	113.4			142.3	153.7	151.7
$^3(\text{Pd}-\text{Bz})^{2+}$	198.4			212.6			165.4			213.3		
$^3(\text{Pt}-\text{Bz})^{2+}$	219.1			236.4			174.3			232.8		
lowest structure MP2/aVDZ	MP2/aVTZ/ MP2/aVDZ			MP2/CBS//MP2/aVDZ			CCSD(T)/aVDZ/ MP2/aVDZ			CCSD(T)/CBS//MP2/aVDZ		
	$\pi_{\text{cent}}(\eta^6)$	$\pi_{\text{c}}(\eta^3)$	$\pi_{\text{off}}(\eta^4)$	$\pi_{\text{cent}}(\eta^6)$	$\pi_{\text{c}}(\eta^3)$	$\pi_{\text{off}}(\eta^4)$	$\pi_{\text{cent}}(\eta^6)$	$\pi_{\text{c}}(\eta^3)$	$\pi_{\text{off}}(\eta^4)$	$\pi_{\text{cent}}(\eta^6)$	$\pi_{\text{c}}(\eta^3)$	$\pi_{\text{off}}(\eta^4)$
$^1(\text{Na}-\text{Bz})^+$		21.7		22.1			22.1			22.1		
$^1(\text{Cu}-\text{Bz})^+$		59.7		62.9			45.4			56.0		
$^1(\text{Ag}-\text{Bz})^+$		40.9		43.5			31.4			40.1		
$^1(\text{Au}-\text{Bz})^+$		69.7		73.1			52.9			64.3		
$^1(\text{Pd}-\text{Bz})^{2+}$		205.5		222.7			157.4			215.4		
$^1(\text{Pt}-\text{Bz})^{2+}$		230.7		251.3			173.8			243.4		
$^1(\text{Hg}-\text{Bz})^{2+}$		143.8		152.8			123.0			153.7		
$^3(\text{Pd}-\text{Bz})^{2+}$		198.4		212.6			165.4			213.3		
$^3(\text{Pt}-\text{Bz})^{2+}$		219.1		236.4			174.3			232.8		
									expt.			
									$22.1 \pm 1.4$			
									$52 \pm 5$			
									$37.4 \pm 1.7$			
									$69 \pm 7$			

<sup>a</sup> The energy was corrected by ZPE. For MP2/aVTZ//MP2/aVDZ, MP2/CBS//MP2/aVDZ, CCSD(T)/aVDZ//MP2/aVDZ, and CCSDT(T)/CBS//MP2/aVDZ calculations, only the binding energies of the most stable structures are collected in this table. For  $^1(\text{Cu}-\text{Bz})^+$  and  $^1(\text{Au}-\text{Bz})^+$ , only the  $\pi_{\text{cent}}(\eta^6)$  conformation is stable at the MP2/aVDZ level (ref 10d). Experimental values are from refs 30–32. For the  $\text{TM}^{2+}$ -Bz complexes, the spin-orbit coupling corrections for the binding energy by using the multiconfiguration calculations are no more than 0.01 kcal/mol due to the calculation of errors, which is not included in this table.

**Table 3.** Calculated Vibrational Frequencies of Benzene<sup>a</sup>

approx. mode	B3LYP	MP2	QCISD	expt.
CH: out-of-plane bending	413 <sub>0</sub>	434 <sub>0</sub>	399 <sub>0</sub>	
CH: out-of-plane bending	679 <sub>112</sub>	746 <sub>116</sub>	685 <sub>112</sub>	673
ring stretching	974 <sub>0</sub>	1066 <sub>0</sub>	976 <sub>0</sub>	992
ring breathing	982 <sub>0</sub>	967 <sub>0</sub>	1012 <sub>0</sub>	
CH: in-plane bending	1024 <sub>6</sub>	1010 <sub>5</sub>	1057 <sub>4</sub>	1038
D-ring: ring distortion	1448 <sub>6</sub>	1411 <sub>5</sub>	1491 <sub>5</sub>	1486
CC: stretching <sup>b</sup>	1584 <sub>0</sub>	1560 <sub>0</sub>	1647 <sub>0</sub>	
CH: stretching	3095 <sub>35</sub>	3101 <sub>28</sub>	3210 <sub>36</sub>	3210

<sup>a</sup> The aVDZ basis set was employed. The experimental values are from ref 33. Frequencies are in cm<sup>-1</sup>, and IR intensities in km/mol are in subscripts. <sup>b</sup> IR inactive; not observed in the experiment (ref 34).

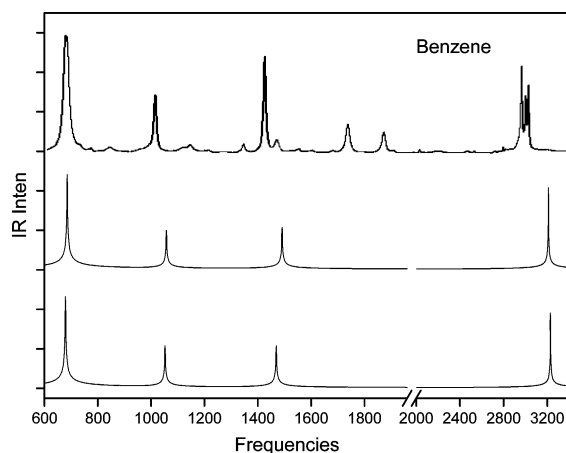


**Figure 3.** IR spectra of benzene [MP2/aVDZ (bottom), QCISD/6-31G\*\* (middle), experiment (top)]. Experimental spectra are from ref 34.

the occupation of “6s” AO of Au<sup>+</sup> in the  $\pi_{\text{cen}}$  conformer is much smaller than the  $\pi_{\text{off}}$  and  $\pi_{\text{C}}$  conformers, indicating that the TM $\leftarrow\pi$  donation from Bz to the unoccupied “s” orbital of Au is less favorable in the  $\pi_{\text{cen}}$  structure.

For the singlet states of the Pd<sup>2+</sup>-Bz and Pt<sup>2+</sup>-Bz complexes, the B3LYP calculations predict that the  $\pi_{\text{off}}$  and  $\pi_{\text{C}}$  structures are isoenergetic, whereas the MP2 calculations show that the  $\pi_{\text{off}}$  conformer is particularly more stable. For the triplet states of Pd<sup>2+</sup> and Pt<sup>2+</sup>, there are two singly occupied AOs with no empty d orbitals. B3LYP, PBE, and CISD predict that in the case of Pd<sup>2+</sup>-Bz complex the triplet  $\pi_{\text{cen}}$  structure is 12 kcal/mol more stable than the singlet  $\pi_{\text{off}}$  and  $\pi_{\text{C}}$  structures. On the other hand, MP2/CBS and CCSD(T)/CBS calculations show that for both Pd<sup>2+</sup>-Bz and Pt<sup>2+</sup>-Bz complexes the singlet  $\pi_{\text{off}}$  ( $\eta^4$ , which is practically similar in shape to  $\eta^2$ ) structures are 17–19 and 24–31 kcal/mol more stable, respectively, than the triplet  $\pi_{\text{cen}}$  structures, which agrees with the observed singlet state of benzene  $\eta^2$  coordinated with Pt<sup>2+</sup> complexes.<sup>15,16</sup> Thus, MP2 calculations are likely to be more reliable than B3LYP, PBE, and CISD, while of course the CCSD(T)/CBS results would be the most reliable. Nevertheless, for more reliable results, the singlet–triplet separation would require multiconfiguration studies, which need to be done in the future. At the CCSD(T)/CBS level, the singlet–triplet splitting is 27.9 kcal/mol for Pd<sup>2+</sup> and 25.4 kcal/mol for Pt<sup>2+</sup> (or 30.6 kcal/mol for Pd<sup>2+</sup> and 30.8 kcal/mol for Pt<sup>2+</sup> after weighted averaging over all of the angular momentum states  $J$ :<sup>10d</sup>  $E_{\text{avg}} = \sum_J [(2J + 1)/(2S +$

$1)(2L + 1)]E_J$ ). However, it may be energetically favorable that an electron promotes from a singly occupied d orbital to another in Pd<sup>2+</sup> or Pt<sup>2+</sup>, which makes it possible a TM $\leftarrow$ ligand donation from an occupied  $\pi$  orbital or a lone electron pair to an empty d orbital of Pd<sup>2+</sup> or Pt<sup>2+</sup> (Figure 5a,b). After Pd<sup>2+</sup> and Pt<sup>2+</sup> interact with Bz, their single states are 2.1 and 10.6 kcal/mol more stable than their respective triplet states, respectively (Table 2).

Molecular dications formed by attachment of a TM<sup>2+</sup> dication to Bz show significant charge transfer, as in Table 4. Although the binding of Pd<sup>2+</sup>, Pt<sup>2+</sup>, or Hg<sup>2+</sup> with Bz is very strong, the intermolecular mode frequency is very small (Table 4), which indicates that the large binding energy of TM<sup>2+</sup> attached to Bz is mainly attributed to the electrostatic interaction, but not covalent bonding. However, the TM $\leftarrow\pi$  donation makes the binding of Pd<sup>2+</sup>/Pt<sup>2+</sup> favor the  $\pi_{\text{off}}$  structure (Figure 5a,b). Because the s–d orbital energy splitting of Hg is very large, the s–d hybridization is not favorable for Hg<sup>2+</sup>, and the “5d” AOs of Hg<sup>2+</sup> are almost fully occupied. For the Hg<sup>2+</sup>-Bz complex, the occupation of “6s” AO on the Hg atom indicates the TM $\leftarrow\pi$  donation from a  $\pi$  MO of Bz to an unoccupied “s” AO of Hg<sup>2+</sup> (Figure 5c). As a result, the TM $\leftarrow\pi$  donation from Bz to the unoccupied “6s” AO of Hg<sup>2+</sup> favors the  $\pi_{\text{C}}$  or  $\pi_{\text{off}}$  structure. The NBO analysis also shows that the occupation of “6s” AO for Hg<sup>2+</sup> in the  $\pi_{\text{cen}}$  structure is much smaller than that of the  $\pi_{\text{C}}$  or  $\pi_{\text{off}}$  structure.

The  $\pi$  complexes of Au<sup>+</sup>, Pd<sup>2+</sup>, Pt<sup>2+</sup>, and Hg<sup>2+</sup> give a few split IR peaks for the C–C stretching modes at about 1600 cm<sup>-1</sup>, and several split IR peaks of the C–H stretching modes. The degenerate C–C stretching vibrations of the pure Bz are IR inactive at 1624 cm<sup>-1</sup>, while they split into two IR active frequencies at 1576 and 1606 cm<sup>-1</sup> for the Au<sup>+</sup>-Bz complex. Because of the delocalization of the  $\pi$  ring, the C–C stretching frequencies are red-shifted as compared to those of Bz. The degenerate carbon ring distortion frequencies of Bz also split into two frequencies, 1446 and 1490 cm<sup>-1</sup>, for the Au<sup>+</sup>-Bz complex. The situation is similar for the  $\pi$  complexes of Pd<sup>2+</sup>, Pt<sup>2+</sup>, and Hg<sup>2+</sup>. For Pd<sup>2+</sup>-Bz, the C–C bond is greatly lengthened. The frequency of the related C–C stretching is also greatly red-shifted. The IR spectrum of the Pt<sup>2+</sup>-Bz complex is similar to that of the Pt<sup>2+</sup>-Bz complex. However, the Pt<sup>2+</sup>-Bz complex gives the C–C stretching mode frequency (1363 cm<sup>-1</sup>). Furthermore, more C–H stretching modes are IR active for Au<sup>+</sup>-, Pd<sup>2+</sup>-, Pt<sup>2+</sup>-, and Hg<sup>2+</sup>-Bz complexes, while the Hg<sup>2+</sup>-Bz complex gives more red-shift in the C–H stretching mode frequency, which is probably correlated to the  $\sigma$  coordination. As shown in Figure 4, the symmetrical C–H stretching vibrational frequencies are split for the cases of the Au<sup>+</sup>, Pd<sup>2+</sup>, Pt<sup>2+</sup>, and Hg<sup>2+</sup> complexes, and, in particular, the splitting for the Hg<sup>2+</sup> complex is very wide.

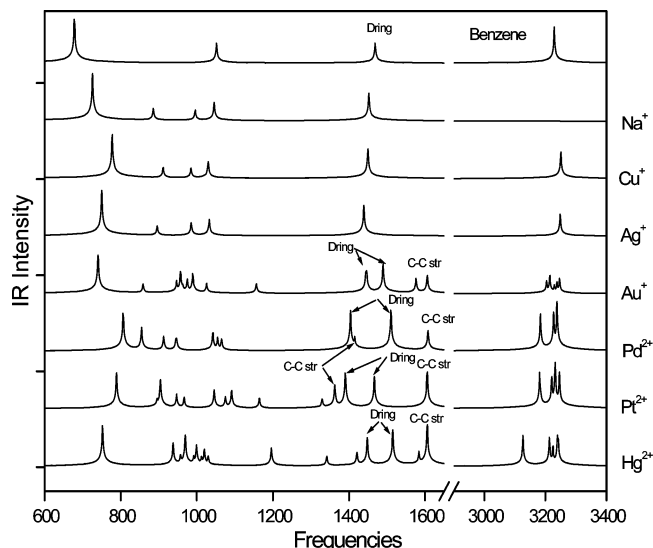
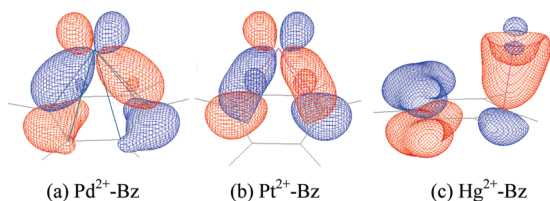
#### IV. Conclusion

We have investigated the conformations and interaction energies of Bz with TM<sup>n+</sup> (Na<sup>+</sup>, Cu<sup>+</sup>, Ag<sup>+</sup>, Au<sup>+</sup>, Pd<sup>2+</sup>,

**Table 4.** Intermolecular Mode Frequencies and Charge Transfer (CT) of the Lowest Energy Structures of the  $\text{TM}^{n+}$ –Bz Complexes<sup>a</sup>

	$^1(\text{Na-Bz})^+$	$^1(\text{Cu-Bz})^+$	$^1(\text{Ag-Bz})^+$	$^1(\text{Au-Bz})^+$	$^1(\text{Pd-Bz})^{2+}$	$^1(\text{Pt-Bz})^{2+}$	$^1(\text{Hg-Bz})^{2+}$
$\omega_i$	193 <sub>35</sub>	224 <sub>2</sub>	186 <sub>6</sub>	297 <sub>0</sub>	278 <sub>11</sub>	379 <sub>36</sub>	252 <sub>0</sub>
$d$	241	170	212	202	163	170	220
CT	0.0	−0.04	0.02	0.21	1.18	1.11	0.63

<sup>a</sup> Frequencies ( $\omega_i$  in  $\text{cm}^{-1}$ ), IR intensities (in  $\text{km/mol}$  in subscripts), and vertical distances from a cation to the Bz plane ( $d$  in pm) were obtained at the MP2/aVDZ level. The amount of CT was obtained in NBO charges at the MP2/aVTZ level.

**Figure 4.** MP2/aVDZ calculated IR spectra of the pure Bz and the  $\text{TM}^{n+}$ –Bz complexes.**Figure 5.** Occupied molecular orbitals of the  $\text{TM}^{2+}$  dication attached to Bz.

$\text{Pt}^{2+}$ , and  $\text{Hg}^{2+}$ ) using B3LYP/aVDZ, PBE/aVDZ, QCISD/6-31G\*\*, MP2/aVDZ, and MP2/aVTZ calculations and MP2/CBS and CCSD(T)/CBS approximations. The CCSD(T)/CBS results agree with the experimental values, in particular, in the binding energies and singlet–triplet energy separation. The QCISD/6-31G\*\* binding energies of  $\text{Na}^+$ –Bz,  $\text{Cu}^+$ –Bz, and  $\text{Ag}^+$ –Bz also agree well with the experimental values, while the QCISD calculations apparently underestimate that of  $\text{Au}^+$ –Bz. For  $\text{TM}^{n+}$ –Bz ( $\text{TM}^{n+} = \text{Pd}^{2+}$ ,  $\text{Pt}^{2+}$ ), MP2 calculations show that the singlet  $\pi$  conformers are more stable than the triplet  $\pi$  conformers. Although the binding of  $\text{Cu}^+$ / $\text{Ag}^+$  with Bz arises mainly from the electrostatic and induction interactions, the binding of  $\text{Au}^+$ ,  $\text{Pd}^{2+}$ ,  $\text{Pt}^{2+}$ , or  $\text{Hg}^{2+}$  with Bz involves significant charge transfer, and the electrostatic interaction still plays a more important role than the covalent bonding. Because of the characteristic binding, the binding sites of the metal cation in the  $\text{Au}^+$ –,  $\text{Pd}^{2+}$ –,  $\text{Pt}^{2+}$ –, and  $\text{Hg}^{2+}$ –Bz complexes depend on the metal. The  $\text{Na}^+$ –,  $\text{Cu}^+$ –, and  $\text{Ag}^+$ –Bz complexes prefer the  $\pi_{\text{cen}}(\eta^6)$  structure of  $C_{6v}$  symmetry. The  $\text{Na}^+$  complex prefers the

$\pi_{\text{cen}}(\eta^6)$  structure of  $C_{6v}$  symmetry. The  $\text{Cu}^+$  and  $\text{Ag}^+$  cations can be over all of the benzene plane, but would still favor the  $\pi_{\text{cen}}(\eta^6)$  structure of  $C_{6v}$  symmetry. The  $\text{Au}^+$ –Bz complex favors the  $\pi_{\text{off}}(\eta^2)$  or  $\pi_{\text{C}}(\eta^1)$  structure, and the  $\text{Pd}^{2+}$ – and  $\text{Pt}^{2+}$ –Bz complexes favor the  $\pi_{\text{off}}(\eta^4)$  structures. The  $\text{Hg}^{2+}$ –Bz complex favors the  $\sigma$  or  $\pi_{\text{C}}(\eta^1)$  structure.

The  $\text{TM}^{n+}$ –Bz complexes give characteristic IR peaks. The MP2/aVDZ calculations show that for the  $\text{Na}^+$ ,  $\text{Cu}^+$ , and  $\text{Ag}^+$  complexes, the out-of-plane bending frequencies are blue-shifted with respect to that of the pure Bz at  $679 \text{ cm}^{-1}$ , and an out-of-plane bending mode and a symmetric ring breathing mode appear at  $800$ – $1000 \text{ cm}^{-1}$ . In contrast to the nonactive C–C stretching mode of the pure Bz and the  $\text{Na}^+$ ,  $\text{Cu}^+$ , and  $\text{Ag}^+$  complexes due to the  $C_6$  symmetry, the C–C stretching modes in the  $\text{Au}^+$ ,  $\text{Pd}^{2+}$ ,  $\text{Pt}^{2+}$ , and  $\text{Hg}^{2+}$  complexes are IR active due to the nonsymmetric geometry. This distinction would be useful to identify the complex symmetry and find the binding site of the metal on the benzene. The  $\text{Au}^+$ –Bz complex shows two IR active frequencies at  $1576$  and  $1606 \text{ cm}^{-1}$ . For the  $\text{Pd}^{2+}$ – and  $\text{Pt}^{2+}$ –Bz complexes, the C–C bond is lengthened, resulting in a large red-shift. The  $\text{Hg}^{2+}$ –Bz complex gives a large red-shift in the C–H stretching frequency due to the  $\sigma$  coordination.

**Acknowledgment.** K.S.K. acknowledges the support from KOSEF (WCU, R32-2008-000-10180-0; EPB Center, R11-2008-052-01000), BK21 (KRF), and GRL (KICOS). H.-B.Y. acknowledges the support by the 985 Project of Hunan University (China). H.M.L. acknowledges the KRF Grant of MOEHRD (Korea) (KRF-2006-353-C00022). The support from the KISTI Supercomputing Center (KSC-2008-K08-0002, KSC-2007-S00-3005) is acknowledged.

## References

- (1) (a) Ma, J. C.; Dougherty, D. A. *Chem. Rev.* **1997**, *97*, 1303–1324. (b) Kumpf, R.; Dougherty, D. A. *Science* **1993**, *261*, 1708–1710. (c) Mecozzi, S.; West, A. P., Jr.; Dougherty, D. A. *J. Am. Chem. Soc.* **1996**, *118*, 2307–2308. (d) Kim, K. S.; Tarakeswar, P.; Lee, J. Y. *Chem. Rev.* **2000**, *100*, 4145–4186. (e) Pullman, A.; Berthier, G.; Savinelli, R. *J. Comput. Chem.* **1997**, *18*, 2012–2022. (f) Kim, K. S.; Lee, J. Y.; Lee, S. J.; Ha, T.-K.; Kim, D. H. *J. Am. Chem. Soc.* **1994**, *116*, 7399–7400. (g) Pierpont, C. G.; Buchanan, R. M. *Coord. Chem. Rev.* **1981**, *38*, 45–87. (h) Singh, N. J.; Min, S. K.; Kim, D. Y.; Kim, K. S. *J. Chem. Theory Comput.* **2009**, *5*, 515–529.
- (2) (a) Cabarcos, O. M.; Weinheimer, C. J.; Lisy, J. M. *J. Chem. Phys.* **1999**, *110*, 8429–8435. (b) Cabarcos, O. M.; Weinheimer, C. J.; Lisy, J. M. *J. Chem. Phys.* **1998**, *108*, 5151–5154.

- (3) Rodgers, M. T.; Armentrout, P. B. *Mass Spectrom. Rev.* **2000**, *19*, 215–247.
- (4) Kim, D.; Hu, S.; Tarakeshwar, P.; Kim, K. S.; Lisy, J. M. *J. Phys. Chem. A* **2003**, *107*, 1228–1238.
- (5) (a) Schröder, D.; Wesendrup, R.; Hertwig, R. H.; Dargel, T. K.; Grauel, H.; Koch, W.; Bender, B. R.; Schwarz, H. *Organometallics* **2000**, *19*, 2608–2615. (b) Kim, D.; Lee, E. C.; Kim, K. S.; Tarakeshwar, P. *J. Phys. Chem. A* **2007**, *111*, 7980–7986. (c) Lee, J. Y.; Lee, S. J.; Choi, H. S.; Cho, S. J.; Kim, K. S.; Ha, T. K. *Chem. Phys. Lett.* **1995**, *232*, 67–71.
- (6) (a) Hu, J.; Barbour, L. J.; Gokel, G. W. *J. Am. Chem. Soc.* **2001**, *123*, 9486–9487. (b) Gokel, G. W.; Barbour, L. J.; Ferdani, R.; Hu, J. *Acc. Chem. Res.* **2002**, *35*, 878–886. (c) Choi, H. S.; Suh, S. B.; Cho, S. J.; Kim, K. S. *Proc. Natl. Acad. Sci. U.S.A.* **1998**, *95*, 12904–12909. (d) McFail-Isom, L.; Shui, X. Q.; Williams, L. D. *Biochemistry* **1998**, *37*, 17105–17111. (e) Zaric, S. D.; Popovic, D. M.; Knapp, E. W. *Chem.-Eur. J.* **2000**, *6*, 3935–3942.
- (7) (a) Hong, B. H.; Lee, J. Y.; Lee, C.-W.; Kim, J. C.; Bae, S. C.; Kim, K. S. *J. Am. Chem. Soc.* **2001**, *123*, 10748–10749. (b) Hong, B. H.; Bae, S. C.; Lee, C.-W.; Jeong, S.; Kim, K. S. *Science* **2001**, *294*, 348–351. (c) Singh, N. J.; Lee, E. C.; Choi, Y. C.; Lee, H. M.; Kim, K. S. *Bull. Chem. Soc. Jpn.* **2007**, *80*, 1437–1450. (d) Singh, N. J.; Lee, H. M.; Suh, S. B.; Kim, K. S. *Pure Appl. Chem.* **2007**, *79*, 1057–1075.
- (8) (a) Oh, K. S.; Lee, C.-W.; Choi, H. S.; Lee, S. J.; Kim, K. S. *Org. Lett.* **2000**, *2*, 2679–2681. (b) Choi, H. S.; Kim, D.; Tarakeshwar, P.; Suh, S. B.; Kim, K. S. *J. Org. Chem.* **2002**, *67*, 1848–1851. (c) Yun, S.; Kim, Y.-O.; Kim, D.; Kim, H. G.; Ihm, H.; Kim, J. K.; Lee, C.-W.; Lee, W. J.; Yoon, J.; Oh, K. S.; Yoon, J.; Park, S.-M.; Kim, K. S. *Org. Lett.* **2003**, *5*, 471–474. (d) Singh, N. J.; Lee, H. M.; Hwang, I.-C.; Kim, K. S. *Supramol. Chem.* **2007**, *19*, 321–332.
- (9) (a) Gapeev, A.; Dunbar, R. C. *J. Am. Chem. Soc.* **2001**, *123*, 8360–8365. (b) Dunbar, R. C. *J. Phys. Chem. A* **2000**, *104*, 8067–8074. (c) Dunbar, R. C. *J. Phys. Chem. A* **1998**, *102*, 8946–8952. (d) Tsuzuki, S.; Yoshida, M.; Uchimaru, T.; Mikami, M. *J. Phys. Chem. A* **2001**, *105*, 769–773. (e) Alberti, M.; Aguilar, A.; Lucas, J. M.; Lagana, A.; Pirani, F. *J. Phys. Chem. A* **2007**, *111*, 1780–1787. (f) Ruan, C. H.; Rodgers, M. T. *J. Am. Chem. Soc.* **2004**, *126*, 14600–14610.
- (10) (a) Polfer, N. C.; Oomens, J.; Morre, D. T.; von Helden, G.; Meijer, G.; Dunbar, R. C. *J. Am. Chem. Soc.* **2006**, *128*, 517–525. (b) Dunbar, R. C.; Moore, D. T.; Oomens, J. *J. Phys. Chem. A* **2006**, *110*, 8316–8326. (c) Moore, D. T.; Oomens, J.; Eyler, J. R.; von Helden, G.; Meijer, G.; Dunbar, R. C. *J. Am. Chem. Soc.* **2005**, *127*, 7243–7254. (d) Yi, H.-B.; Diefenbach, M.; Choi, Y. C.; Lee, E. C.; Lee, H. M.; Hong, B. H.; Kim, K. S. *Chem.-Eur. J.* **2006**, *12*, 4885–4892. (e) Pandey, R.; Rao, B. K.; Jena, P.; Blanco, M. A. *J. Am. Chem. Soc.* **2001**, *123*, 3799–3808. (f) Roszak, S.; Balasubramanian, K. *Chem. Phys. Lett.* **1995**, *234*, 101–106.
- (11) Nazin, G. V.; Qiu, X. H.; Ho, W. *Science* **2003**, *302*, 77–81.
- (12) Dargel, T. K.; Hertwig, R. H.; Koch, W. *Mol. Phys.* **1999**, *96*, 583–592.
- (13) Petrie, S.; Radom, L. *Int. J. Mass Spectrom.* **1999**, *192*, 173–183.
- (14) Alcamí, M.; González, A. I.; Mó, O.; Yáñez, M. *Chem. Phys. Lett.* **1999**, *307*, 244–252.
- (15) Johansson, L.; Tilst, M.; Labinger, J. A.; Bercaw, J. E. *J. Am. Chem. Soc.* **2000**, *122*, 10486–10487.
- (16) (a) Norris, C. M.; Reinartz, S.; White, P. S.; Templeton, J. L. *Organometallics* **2002**, *21*, 5649–5656. (b) Reinartz, S.; White, P. S.; Brookhart, M.; Templeton, J. L. *J. Am. Chem. Soc.* **2001**, *123*, 12724–12725.
- (17) Siu, F. M.; Ma, N. L.; Tsang, C. W. *J. Am. Chem. Soc.* **2001**, *123*, 3397–3398.
- (18) (a) Nechaev, M.; Rayón, V.; Frenking, G. *J. Phys. Chem. A* **2004**, *108*, 3134–3142. (b) Lupinetti, A. J.; Fau, S.; Frenking, G.; Strauss, S. H. *J. Phys. Chem. A* **1997**, *101*, 9551–9559.
- (19) (a) Sievers, M. R.; Jarvis, L. M.; Armentrout, P. B. *J. Am. Chem. Soc.* **1998**, *120*, 1891–1899. (b) Corral, I.; Mo, O.; Yanez, M. *J. Phys. Chem. A* **2003**, *107*, 1370–1376.
- (20) Pople, J. A.; Head-Gordon, M. *J. Chem. Phys.* **1987**, *87*, 5968–5975.
- (21) (a) Bergner, A.; Dolg, M.; Kuechle, W.; Stoll, H.; Preuss, H. *Mol. Phys.* **1993**, *80*, 1431–1441. (b) Kaupp, M.; Schleyer, P. v. R.; Stoll, H.; Preuss, H. *J. Chem. Phys.* **1991**, *94*, 1360–1366. (c) Dolg, M.; Wedig, U.; Stoll, H.; Preuss, H. *J. Chem. Phys.* **1987**, *86*, 866–872. (d) Dolg, M.; Stoll, H.; Preuss, H.; Pitzer, R. M. *J. Phys. Chem.* **1993**, *97*, 5852–5859.
- (22) Feller, D.; Glendening, E. D.; de Jong, W. A. *J. Chem. Phys.* **1999**, *110*, 1475–1491.
- (23) Matin, J. M. L.; Sundermann, A. *J. Chem. Phys.* **2001**, *114*, 3408–3420.
- (24) (a) Helgaker, T.; Klopper, W.; Koch, H.; Noga, J. *J. Chem. Phys.* **1997**, *106*, 9639–9646. (b) Min, S. K.; Lee, E. C.; Lee, H. M.; Kim, D. Y.; Kim, D.; Kim, K. S. *J. Comput. Chem.* **2008**, *29*, 1208–1221.
- (25) Frisch, M. J.; Trucks, G. W.; Schlegel, H. B.; Scuseria, G. E.; Robb, M. A.; Cheeseman, J. R.; Zakrzewski, V. G.; Montgomery, J. A., Jr.; Stratmann, R. E.; Burant, J. C.; Dapprich, S.; Millam, J. M.; Daniels, A. D.; Kudin, K. N.; Strain, M. C.; Farkas, O.; Tomasi, J.; Barone, V.; Cossi, M.; Cammi, R.; Mennucci, B.; Pomelli, C.; Adamo, C.; Clifford, S.; Ochterski, J.; Petersson, G. A.; Ayala, P. Y.; Cui, Q.; Morokuma, K.; Salvador, P.; Dannenberg, J. J.; Malick, D. K.; Rabuck, A. D.; Raghavachari, K.; Foresman, J. B.; Cioslowski, J.; Ortiz, J. V.; Baboul, A. G.; Stefanov, B. B.; Liu, G.; Liashenko, A.; Piskorz, P.; Komaromi, I.; Gomperts, R.; Martin, R. L.; Fox, D. J.; Keith, T.; Al-Laham, M. A.; Peng, C. Y.; Nanayakkara, A.; Challacombe, M.; Gill, P. M. W.; Johnson, B.; Chen, W.; Wong, M. W.; Andres, J. L.; Gonzalez, C.; Head-Gordon, M.; Replogle, E. S.; Pople, J. A. *Gaussian 03*, revision B.01; Gaussian, Inc.: Pittsburgh, PA, 2003.
- (26) Lee, S. J.; Chung, H. Y.; Kim, K. S. *Bull. Korean Chem. Soc.* **2004**, *25*, 1061–1064.
- (27) (a) Lide, D. R., Ed. *Handbook of Chemistry and Physics*, 1992; 73rd ed., CRC Press Ltd.: Boca Raton, FL, pp 10–211. (b) Bilodeau, R. C.; Scheer, M.; Haugen, H. K. *J. Phys. B: At. Mol. Opt.* **1998**, *31*, 3885–3891. (c) Gantefor, G.; Kraus, S.; Eberhardt, W. *J. Electron Spectrosc. Relat. Phenom.* **1998**, *88*, 35–40. (d) Scheer, M.; Brodie, C. A.; Bilodeau, R. C.; Haugen, H. K. *Phys. Rev. A* **1998**, *58*, 2051–2062. (e) Bilodeau, R. C.; Scheer, M.; Haugen, H. K.; Brooks, R. L. *Phys. Rev. A* **2000**, *61*, 012505-1–012505-7.
- (28) Solcà, N.; Dopfer, O. *Angew. Chem., Int. Ed.* **2002**, *41*, 3628–3631.
- (29) (a) Nicholas, J. B.; Hay, B. P.; Dixon, D. A. *J. Phys. Chem. A* **1999**, *103*, 1394–1400. (b) Feller, D. *Chem. Phys. Lett.* **2000**, *322*, 543–548. (c) Pullman, A.; Berthier, G.; Savinelli, R. *J. Mol. Struct. (THEOCHEM)* **2001**, *537*, 163–172.



- (30) Amicangelo, J. C.; Armentrout, P. B. *J. Phys. Chem. A* **2000**, *104*, 11420–11432.
- (31) (a) Meyer, F.; Khan, F. A.; Armentrout, P. B. *J. Chem. Soc.* **1995**, *117*, 9740–9748. (b) Chen, Y.-M.; Armentrout, P. B. *Chem. Phys. Lett.* **1993**, *210*, 123–128. (c) Rodgers, M. T.; Armentrout, P. B. *J. Phys. Chem. A* **1997**, *101*, 1238–1249. (d) Andersen, A.; Muntean, F.; Walter, D.; Rue, C.; Armentrout, P. B. *J. Phys. Chem.* **2000**, *104*, 692–705.
- (32) Guo, B. C.; Purnell, J. W.; Castleman, A. W., Jr. *Chem. Phys. Lett.* **1990**, *168*, 155–160.
- (33) (a) Jaeger, T. D.; van Heijnsbergen, D.; Klippenstein, S. J.; von Helden, G.; Meijer, G.; Duncan, M. A. *J. Am. Chem. Soc.* **2004**, *126*, 10981–10991. (b) van Heijnsbergen, D.; von Helden, G.; Meijer, G.; Maitre, P.; Duncan, M. A. *J. Am. Chem. Soc.* **2002**, *124*, 1562–1563.
- (34) Kinugasa, S.; Tanabe, K.; Tamura, T. *Spectral Database for Organic Compounds*; National Institute of Advanced Industrial Science and Technology (AIST): Japan.
- (35) Turner, D. W.; Baker, C.; Baker, A. D.; Brundle, C. R. *Molecular Photoelectron Spectroscopy*; Wiley: New York, 1970.
- (36) Shannon, R. D. *Acta Crystallogr.* **1976**, *A32*, 751–767. CT900154X